

SYNOPSIS

The last two decades have seen extensive growth in interest in metal-ion assemblies, especially for building new polynuclear exchange-coupled magnetic systems. However, the concept of designing polynuclear extended structures has still not matured to the level of retrosynthetic approach developed for the organic and pharmacological molecules. Although some progress has been made with secondary building units (SBUs) in metal-organic-frameworks (MOFs), the control seems to be just an illusion when it comes to bridging ligands such as the azide ion. When it is asserted that the azido ligand is versatile in its bridging capabilities, what is actually meant is that it would be difficult to predict or control its bridging properties, or in other words, the azido based polynuclear complexes are difficult to pre-design. However, this kind of serendipity is not always bad news for the chemists. For example, the azido ligand has been shown to mediate magnetic exchanges between paramagnetic metals in a predictable fashion (usually depending upon the bonding geometries). Therefore, it is a well-respected ligand in polynuclear assemblies of paramagnetic ions. Serendipitous assemblies offer new magnetic structures that we may not otherwise even think about synthesizing. Similarly, there are other ligands, such as alkoxido, oximato, carboxylato *etc.* which also behave like azide. These ligands are very important in the study of magnetic exchanges to develop an understanding of the underlying mechanisms in molecular magnetism. Serendipitous assemblies have also led to systems like single molecule magnets (SMMs), which have enriched the field with potential applications in computing and have also been used for the confirmation of the quantum magnetic properties like tunneling phenomenon, spin decoherence *etc.*

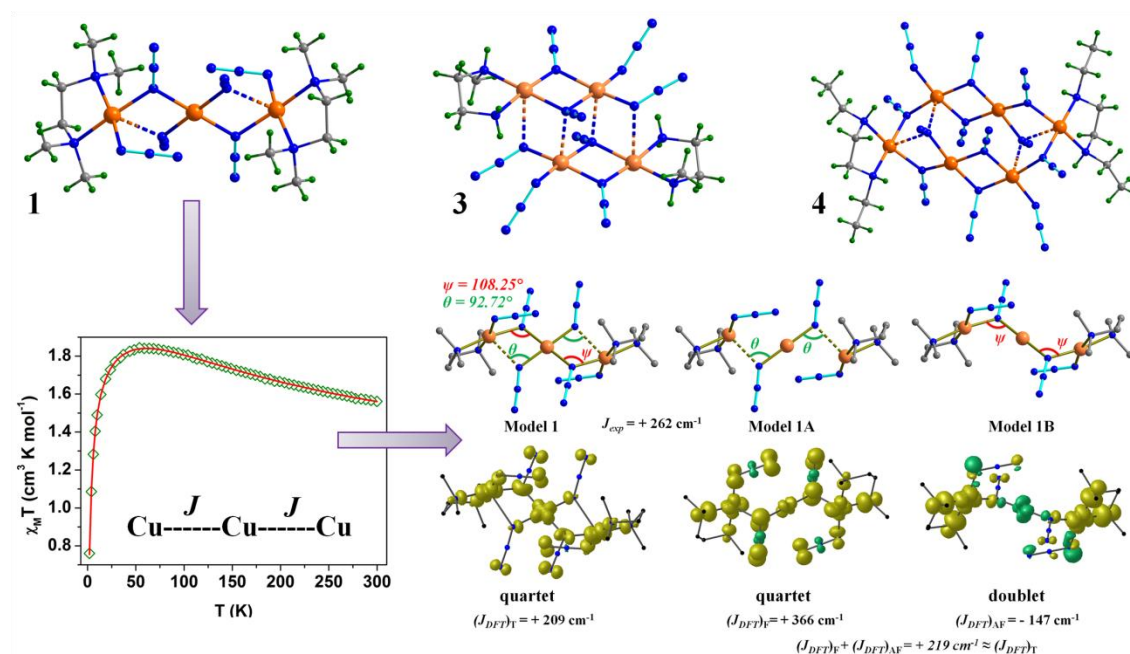
Investigations incorporated in this thesis work led to several novel strategies for using serendipity as an advantage and build unprecedented structural topologies with interesting new molecular-magnetic properties. All the reported complexes were thoroughly analyzed through elemental analysis, spectroscopy, X-ray structure determination (both single crystal & powder diffractions) and variable temperature magnetic susceptibility measurements. In a few suitable cases, model structures obtained from the X-ray structures were also employed to study the magnetic exchange mechanisms through density functional theory (DFT) calculations and simulations.

CHAPTER 1 of the thesis presents a general review on the ever-growing field of metal-ion assembly. In particular, the importance of the ‘serendipitous approach’ to build new and

Synopsis

interesting metal-ion clusters and polyclusters is highlighted. This chapter also describes the basic concepts of exchange-based molecular magnetism as applied to the metal-ion assemblies.

CHAPTER 2 describes the concept of using lower molar proportions of blocking bidentate chelating ligands in the neutral copper(II)-azido systems, which increases the number of coordination sites for the versatile azido bridges to assemble the metal-ions in higher dimensions, based on smaller cluster units. Syntheses, structures and magnetic properties of ten novel complexes are described in this chapter: $[\text{Cu}_3(\text{tmen})_2(\text{N}_3)_6]_n$ (**1**), $[\text{Cu}_4(\text{Me-hmpz})_2(\text{N}_3)_8]_n$ (**2**), $[\text{Cu}_4(\text{men})_2(\text{N}_3)_8]_n$ (**3**), $[\text{Cu}_6(\text{deen})_2(\text{N}_3)_{12}]_n$ (**4**), $[\text{Cu}_6(\text{aem})_2(\text{N}_3)_{12}]_n$ (**5**), $[\text{Cu}_6(\text{dmeen})_2(\text{H}_2\text{O})_2(\text{N}_3)_{12}]_n$ (**6**), $[\text{Cu}_6(\text{N},\text{N}'\text{-dmen})_2(\text{N}_3)_{12}]_n$ (**7**), $[\text{Cu}_6(\text{hmpz})_2(\text{N}_3)_{12}]_n$ (**8**), $[\text{Cu}_5(\text{N},\text{N}\text{-dmen})_2(\text{N}_3)_{10}]_n$ (**9**), and $[\text{Cu}_5(\text{N},\text{N}'\text{-dmen})_5(\text{N}_3)_{10}]_n$ (**10**) [tmen = *N,N,N',N'*-tetramethylethylenediamine, Me-hmpz = 1-methylhomopiperazine, men = *N*-methylethylenediamine, deen = *N,N'*-diethylethylenediamine, aem = 4-(2-aminoethyl)morpholine, dmeen = *N,N*-dimethyl-*N'*-ethylethylenediamine, *N,N'*-dmen = *N,N'*-dimethylethylenediamine, hmpz = homopiperazine, *N,N*-dmen = *N,N*-dimethylethylenediamine].



Scheme 1: Schematic presentation of the basic building units of a few complexes in Chapter 2, along with the magnetic property and DFT analysis for complex 1. [Color codes: Cu, orange; N, blue; C, gray; H, olive.]

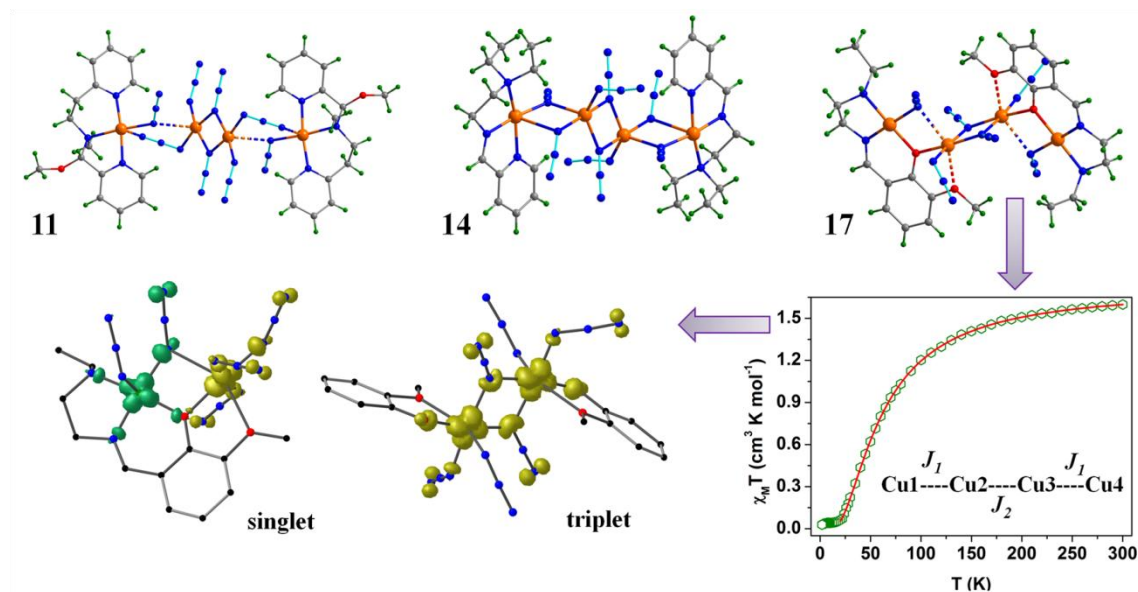
Most of these complexes have simple oligonuclear basic building units (Scheme 1), such as trinuclear (**1**), tetranuclear (**2**, **3**) and hexanuclear (**4-8**), but the overall arrangements of these cluster units in higher dimensions vary widely and serendipitously. For example, the hexanuclear complexes **4-7**, although having almost identical basic structures, assemble in three- (**4**, **5**) or two- (**6**, **7**) dimensions with different connectivity among the basic structures. However, complex **9** is made from two different building units (Cu_2 and Cu_3). Complex **10**, although having metal to blocking molar ratio 1:1, presents an unprecedented 1D structure for such complexes. Analysis of the magnetic susceptibility data for complexes **1-9** using theoretical exchange models for fitting is also described. Density functional theory (DFT, B3LYP) was employed to further analyze the experimental magnetic data for complexes **1**, **2**, **3** and **9** to better understand the magnetic exchange mechanisms in such systems.

CHAPTER 3 continues with the same concepts developed in the previous chapter using multidentate neutral and anionic co-ligands. Using lower molar proportions of these multidentate ligands, seven novel complexes have been synthesized (keeping the initial metal to ligand ratio as 2:1): $[\text{Cu}_4(\text{L}^1)_2(\text{N}_3)_8]_n$ (**11**), $[\text{Cu}_4(\text{L}^2)_2(\text{N}_3)_8]_n$ (**12**), $[\text{Cu}_4(\text{L}^3)_2(\text{N}_3)_8]_n$ (**13**), $[\text{Cu}_4(\text{L}^4)_2(\text{N}_3)_8]_n$ (**14**), $[\text{Cu}_9(\text{L}^5)_4(\text{N}_3)_{18}]_n$ (**15**), $[\text{Cu}_4(\text{L}^6)_2(\text{H}_2\text{O})_2(\text{N}_3)_6]$ (**16**) and $[\text{Cu}_4(\text{L}^7)_2(\text{N}_3)_6]_n$ (**17**) [where L^{1-5} are the condensation products of 2-pyridinecarboxaldehyde and 2-{2-(methylamino)ethyl}pyridine (L^1), *N,N*-diethylethylenediamine (L^2), *N,N*-dimethylethylenediamine (L^3), *N*-methylethylenediamine (L^4), *N,N*,2,2-tetramethylpropanediamine (L^5); HL^6 and HL^7 are the condensation products of 2-hydroxy-3-methoxybenzaldehyde with *N,N*-diethylethylenediamine (HL^6), and *N*-ethylethylenediamine (HL^7)]. The ligand L^1 is particularly interesting, as it is a hemiaminal ether (usually considered to be unstable intermediates in the reactions of aldehydes and secondary amines in alcoholic solvents), and was found to be trapped in **11**. Although **11-13** have identical tetranuclear basic structures (with the rare simultaneous end-on and end-to-end bridges between two neighbouring metal-ions, Scheme 2) and extend in one-dimension. However, **13** is differently organized from the other two complexes. For **14**, the bridging structure among the peripheral copper(II) ions changes to double end-on (Scheme 2), and the resulting structure extends in two dimensions. However, with L^5 , metal to ligand ratio is 9:4 (under similar conditions and initial molar proportions of the components) in **15**, which can be seen as two different fragments: $[\text{Cu}_4(\text{L}^5)_4(\text{N}_3)_6]^{2+}$ and $[\text{Cu}_5(\text{N}_3)_{12}]^{2-}$ linked alternately to give an overall 1D structure. HL^6 and HL^7 have one ionisable phenolic group that replaces one azido anion and

Synopsis

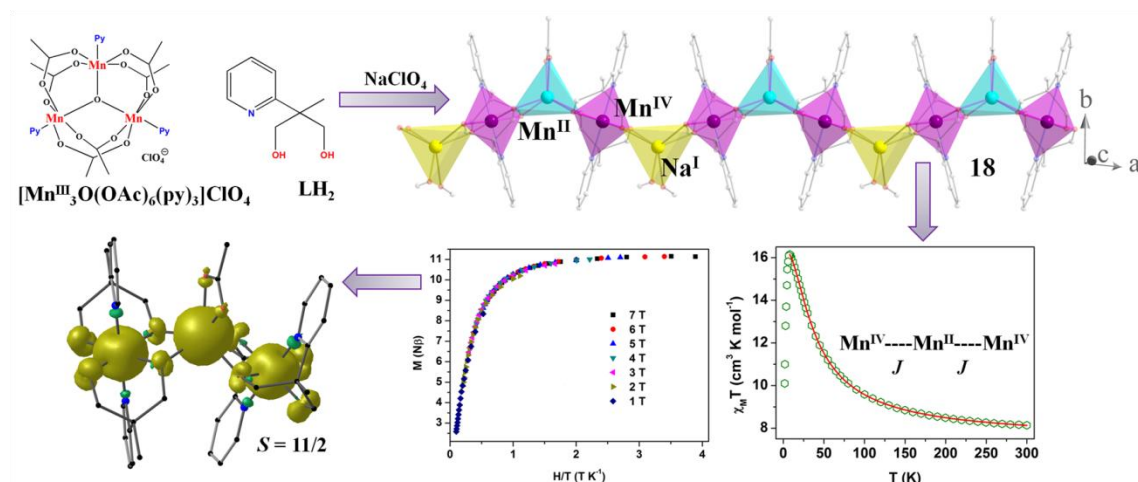
generates two pockets for the metal atoms. These monoanionic ligands give tetranuclear complexes (**16** and **17**) with basic structures resembling (Scheme 2) to **11-14**. While **17** is 1D in nature, two coordinated water molecules prevent the structure of **16** to grow and results in a discrete cluster.

The variable temperature magnetic properties of these complexes were thoroughly analyzed through experimental and theoretical (DFT) studies.



Scheme 2: Schematic presentation of the basic building units of a few complexes in Chapter 3, along with the magnetic property and DFT analysis for complex **17**. [Color codes: Cu, orange; N, blue; O, red; C, gray; H, olive.]

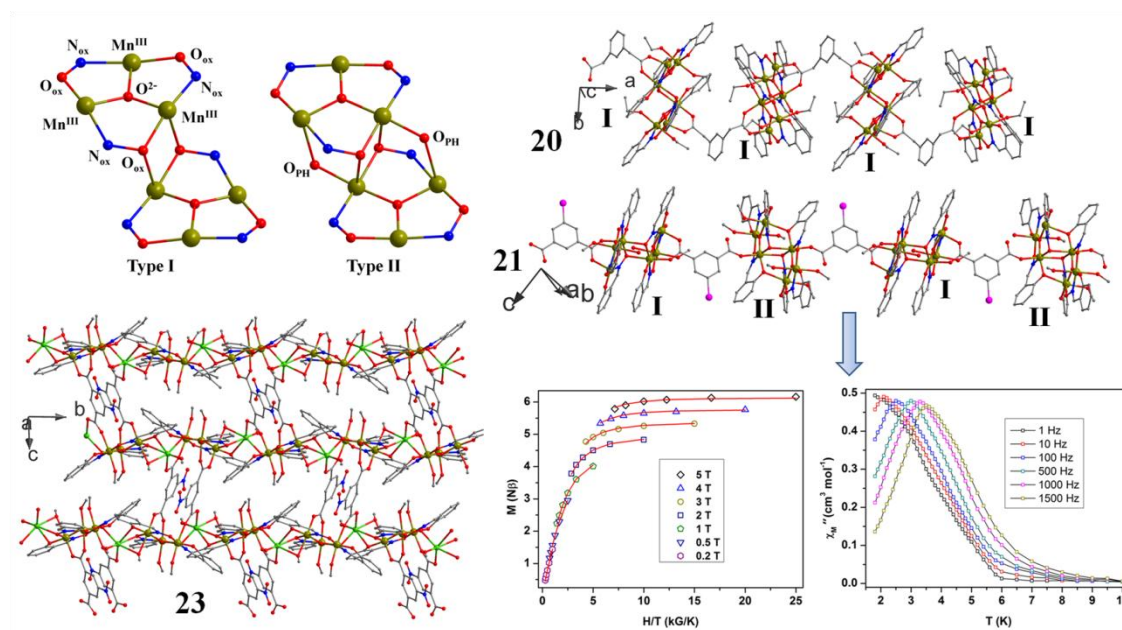
CHAPTER 4 reports the use of a pyridyl substituted propanediolate ligand in the assembly of two novel 1D heterometallic complexes: $[\text{Mn}_3\text{Na}(\text{L})_4(\text{CH}_3\text{CO}_2)(\text{MeOH})_2](\text{ClO}_4)_2 \cdot 3\text{H}_2\text{O}$ (**18**) and $[\text{Mn}_3\text{Na}(\text{L})_4(\text{CH}_3\text{CH}_2\text{CO}_2)(\text{MeOH})_2](\text{ClO}_4)_2 \cdot 2\text{MeOH} \cdot \text{H}_2\text{O}$ (**19**) [LH_2 = 2-methyl-2-(2-pyridyl)propane-1,3-diol, Scheme 3]; both featuring octahedral Mn^{IV} ions linked alternately to one trigonal prismatic Mn^{II} ion and even more interestingly to one trigonal prismatic Na^{I} ion (Scheme 3). The complexes are essentially identical in structure and magnetic behavior, showing a weak ferromagnetic interaction among the neighboring manganese ions. DFT studies on a model complex supports the $S = 11/2$ ground spin state, deduced from *dc* and *ac* susceptibility measurements.



Scheme 3: Schematic presentation for the synthesis of the heteronuclear 1D complex **18** and its magnetic behavior, with the calculated spin ground state.

CHAPTER 5 illustrates the use of a few dicarboxylates as potential bridging ligands to assemble tri- and hexanuclear Mn^{III} -clusters. With the salicylaldoximate (salox) as the $[\text{Mn}^{\text{III}}_3\text{O}(\text{salox})_3]^+$, triangle-generating moiety and keeping the reaction conditions (solvent, base, reaction time and crystallization process) identical, four new extended complexes that differ both in their basic and higher dimensional organizations are reported. When 1,3-phenylenediacetate (phda) is used (in EtOH), in the resulting complex $[\text{Mn}^{\text{III}}_6\text{O}_2(\text{salox})_6(\text{EtOH})_4(\text{phda})]_n \cdot (\text{saloxH}_2)_n \cdot (2\text{H}_2\text{O})_n$ (**20**), a single type of Mn^{III}_6 clusters are linked by the dicarboxylate (interestingly the complex crystallizes with uncoordinated saloxH_2 molecules). However, when two differently substituted isophthalate linkers (5-iodoisophthalate and 5-azidoisophthalate) are used, two almost identical complexes $[\text{Mn}^{\text{III}}_6\text{O}_2(\text{salox})_6(\text{MeOH})_5(5\text{-I-isoph})]_n \cdot (3\text{MeOH})_n$ (**21**) and $[\text{Mn}^{\text{III}}_6\text{O}_2(\text{salox})_6(\text{MeOH})_4(\text{H}_2\text{O})(5\text{-N}_3\text{-isoph})]_n \cdot (4\text{MeOH})_n$ (**22**) are isolated, with two different types of Mn_6 clusters (Scheme 4) linked alternately in one dimension. More interestingly, use of another substituted isophthalate (5-nitroisophthalate) produced a heteronuclear complex $[\text{Mn}^{\text{III}}_3\text{NaO}(\text{salox})_3(\text{MeOH})_4(5\text{-NO}_2\text{-isoph})]_n \cdot (\text{MeOH})_n(\text{H}_2\text{O})_n$ (**23**) with only Mn^{III}_3 triangles as the basic cluster assembled in two dimensions. Temperature and field dependent dc and ac susceptibility measurements show that the complexes **20-22** behave as non-interacting single molecule magnets with ground spin state $S = 4$. Complex **23** is dominantly antiferromagnetic with a ground spin state $S = 2$. The magnetic behaviours of these complexes are also supported by theoretical calculations (DFT) on models generated from the crystal structures.

Synopsis



Scheme 4: Schematic presentation of the different 1D arrangements of hexanuclear Mn^{III} -salicylaldoximate cluster based complexes and their magnetic properties along with the 2D structure of **23**.